International Journal of Control
Publication details, including instructions for authors and subscription information:
http://www.informaworld.com/smpp/title~content=t713393989

Switched linear model predictive controllers for periodic exogenous signals

Liuping Wang[a]; Peter Gawthrop[b]; David. H. Owens[c]; Eric Rogers[d]
[a] School of Electrical and Computer Engineering, RMIT University, Melbourne, Victoria 3000, Australia [b] Department of Mechanical Engineering, University of Glasgow, Glasgow, G12 8QQ, UK [c] Department of Automatic Control and Systems Engineering, University of Sheffield, Sheffield, S1 3JD, UK [d] School of Electronics and Computer Science, University of Southampton, Southampton, SO17 1BJ, UK

Online publication date: 16 March 2010

To cite this Article Wang, Liuping , Gawthrop, Peter , Owens, David. H. and Rogers, Eric(2010) 'Switched linear model predictive controllers for periodic exogenous signals', International Journal of Control, 83: 4, 848 — 861
To link to this Article: DOI: 10.1080/00207170903460501
URL: http://dx.doi.org/10.1080/00207170903460501

International Journal of Control
Vol. 83, No. 4, April 2010, 848–861

Taylor & Francis
Taylor & Francis Group

Switched linear model predictive controllers for periodic exogenous signals

Liuping Wang[a]*, Peter Gawthrop[b], David. H. Owens[c] and Eric Rogers[d]

[a]*School of Electrical and Computer Engineering, RMIT University, Melbourne, Victoria 3000, Australia;* [b]*Department of Mechanical Engineering, University of Glasgow, Glasgow, G12 8QQ, UK;* [c]*Department of Automatic Control and Systems Engineering, University of Sheffield, Sheffield, S1 3JD, UK;* [d]*School of Electronics and Computer Science, University of Southampton, Southampton, SO17 1BJ, UK*

(*Received 11 August 2009; final version received 3 November 2009*)

This article develops switched linear controllers for periodic exogenous signals using the framework of a continuous-time model predictive control. In this framework, the control signal is generated by an algorithm that uses receding horizon control principle with an on-line optimisation scheme that permits inclusion of operational constraints. Unlike traditional repetitive controllers, applying this method in the form of switched linear controllers ensures bumpless transfer from one controller to another. Simulation studies are included to demonstrate the efficacy of the design with or without hard constraints.

Keywords: periodic set-point signal; periodic disturbance; predictive control; constrained control; optimisation

1. Introduction

Control system applications in mechanical systems, manufacturing systems and aerospace systems often require set-point following of a periodic trajectory or signal. These signals have known frequencies and amplitudes but unknown phase information. Another type of control problem often encountered is the rejection of periodic disturbances, where typically the frequency information relating to the disturbance is available either through experimental data analysis or understanding of the system. In both situations, the design of a control system that has the capability to produce zero steady-state error is paramount. Instead of a single frequency in the periodic signal, it is more common in industrial applications that the frequency of the external signal changes with respect to time, such as the trajectory of a cutting tool in machining, or that of an unmanned vehicle. In the situation where a complex trajectory is followed by the feedback control system, the command signal is often decomposed into a piece-wise periodic signal with varying frequencies, and the control system must follow the piece-wise periodic signal with zero steady-state error and with a smooth transition from one signal to another.

Repetitive control is a mature field and Li, Dongchun, and Xianyi (2004) give a comprehensive survey. There are two broad classes of repetitive control: those using external models and those using internal models. The methods using external models include those based on basis functions (Hu and Tomizuka 1993) and disturbance observers (Tomizuka, Chew, and Yang 1990); as the name suggests, a model of the disturbance is used outside a feedback control loop. On the other hand, the internal model approach is explicitly related to the internal model principle (Francis and Wonham 1976) and includes a model of the disturbance within the feedback loop.

It is well known from the internal model control principle that in order to reject a periodic disturbance, or follow a periodic reference signal with zero steady-state error, the generator for the disturbance or the reference must be included in the stable closed-loop control system (Francis and Wonham 1976). The most commonly known control systems that reject periodic disturbance and follow a periodic reference signal are the repetitive control systems and these use the internal model control principle (see e.g. Hara, Yamamoto, Omata, and Nakano 1988; Manayathara, Tsao, Bentsman, and Ross 1996; Bai and Wu 1998; Owens, Li, and Banks 2004). In the design of periodic repetitive control systems, the control signal is often generated by a controller that is explicitly described by a transfer function with appropriate coefficients (Hara et al. 1988; Owens et al. 2004). If there are a number of frequencies contained in the exogenous signal, all periodic modes will be contained in the system which is then of higher order (Owens et al. 2004).

Instead of containing all the periodic modes in the periodic control system, an alternative is to embed fewer periodic modes at a given time, and when the

*Corresponding author. Email: liuping.wang@rmit.edu.au

ISSN 0020–7179 print/ISSN 1366–5820 online

DOI: 10.1080/00207170903460501
http://www.informaworld.com

frequency of the external signal changes, the coefficients of the controller change accordingly. This will effectively result in a lower order system by using the strategy of switched linear controllers. Apart from knowing which periodic controller should be used, no bump occurring in the control signal, when switching from one controller to another, is paramount from implementation point of view. In the steady-state, a control signal with a periodic exogenous signal is also periodic, and in a transfer-function-based repetitive control system difficulties could arise in ensuring bumpless transfer from one linear periodic controller to another.

Although the issue of saturating actuators has been studied in the context of repetitive control (Sbarbaro, Tomizuka and Leon de la Barra 2009), the natural setting for constrained control is model based predictive control. This article develops linear switched controllers for periodic exogenous signals using the framework of continuous-time model predictive control. For a continuous-time model predictive control system, the control signal is generated by a control algorithm using receding horizon control principle with an on-line optimisation scheme (see e.g. Wang 2009). This has the advantages over alternative repetitive controllers when employed in the form of switched linear controllers. Moreover, this advantage becomes more evident when bumpless transfer from one linear periodic controller to another is required.

The majority of the development of model predictive control in the past few decades has been based on discrete-time models (see e.g. Maciejowski 2002; Rawlings 2000). The continuous-time model predictive control design using state-space models has emerged in the recent years (see e.g. Wang 2001, 2009; Gawthrop and Ronco 2002), and this setting brings a number of advantages, one of which is less sensitivity to the choice of sampling interval. In a fast sampling environment, a continuous-time model outperforms its discrete counter-part in terms of numerical stability (Garnier and Wang 2008). Additionally, there is some flexibility to cope with systems where there are irregular sampling and event sampling environments (Gawthrop and Wang 2009). Moreover, intermittent predictive control offers additional flexibility in the implementation of continuous-time model predictive control (Gawthrop and Wang 2006).

There are three considerations in the design of a switched model predictive controller for periodic exogenous signals. Firstly, the input disturbance in a state-space model is assumed to be periodic and consequently a periodic disturbance model is naturally incorporated into an augmented design model to satisfy the internal model control principle. Secondly, the signal to be optimised in the scheme is the control signal filtered by the inverse periodic disturbance model, and the control signal itself is constructed iteratively using the optimised signal to ensure the near continuity of the control signal when switched from one periodic controller to another. This differs from the other approaches in the literature, such as repetitive control and other optimal control systems (see e.g. Owens et al. 2004; Nestorovic-Trajkov, Koppe, and Gabbert 2005) in which the control signal itself is optimised, and as a result, the continuity of the control signal could be violated when switched from one controller to another.

Thirdly, a continuous-time predictive control system is used in the design and the discretisation occurs at the implementation stage, which permits fast sampling rate and effectively reduces the transient error when the controller is switched. With continuous-time model predictive control, two different cost functions are used before and after the switch, and because of the fast sampling rate and bumpless transfer, the error signal due to the switch can be made as small as possible by reduction of the sampling interval (Nestorovic-Trajkov et al. 2005).

The central idea of the design method developed in this article is to use a set of Laguerre exponential functions to describe the control trajectory, based on the approach used first by Wang (2001) (for a more detailed treatment see Wang (2009)). However, because the focus is on periodic signals, a set of continuous-time Laguerre functions, which are orthogonal, are used to describe the filtered control signal and the filter is the inverse of the disturbance model. Hence the optimal control trajectory of the predictive control is captured by the coefficients of the Laguerre polynomials and the set of known Laguerre exponential functions. In the cost function, the errors comprise two components, the first one being the error between the desired and actual derivatives of output, whilst the second is the error between the desired and actual outputs. The predictive control problem is converted to a real-time optimisation problem that finds the optimal Laguerre coefficients subject to constraints. Since the control system here is designed using receding horizon control principle, the operational constraints, such as the limits on the derivatives and amplitude of the control signal, are systematically imposed in the design. The results in this article also show that when the constraints become activated, the predictive control system produces optimal results. Conversely, the simulation studies demonstrate that if saturation of the control input is enforced without this mechanism, the control performance degrades significantly.

This article is organised as follows. In Section 2, the continuous-time model predictive control algorithm for periodic exogenous signals is developed; in

addition, constraints and implementation of the switched linear controller are considered; in Section 3, extensive simulation studies of set-point following and disturbance rejection of piece-wise periodic signals, with or without constraints, are presented and discussed. In Section 4, simulation results from a gantry robot is shown to track a desired trajectory in an operational mode where the model used is constructed from measured frequency response data.

2. Control algorithm design

Suppose that the plant to be controlled is described by the state-space model:

$$\dot{x}_m(t) = A_m x_m(t) + B_m u(t) + \Omega_m \mu(t) \tag{1}$$

$$y(t) = C_m x_m(t) \tag{2}$$

where $x_m(t)$ is the $n_1 \times 1$ state vector, $u(t)$ is the input vector, $y(t)$ the output vector, both of which are $r \times 1$ vectors, and $\mu(t)$ represents input disturbance vector. For simplicity of notation, we first assume that the plant is single-input and single-output.

In previous work, by assuming that the input disturbance $\mu(t)$ was a source of integrated white noise, the predictive controller has an integrator naturally embedded in its structure (Clarke, Mohtadi, and Tuffs (1987) for the discrete case, and Wang (2001) for the continuous-time case). Here, we follow a similar route to develop predictive control systems that have the capability to reject periodic input disturbances. As a consequence, the resulting predictive control schemes will also follow the same type of input signals with zero steady-state errors.

2.1 *Development of design model*

Assume that the Laplace transform of the denominator of the disturbance model is of the form

$$D(s) = s^\gamma + d_1 s^{\gamma-1} + d_2 s^{\gamma-2} + \cdots + d_\gamma \tag{3}$$

where the roots of polynomial $D(s)$ are either on the imaginary axis or in the open left-half of the complex plane. When the disturbance has multi-periodicity with known frequencies $\omega_1, \omega_2, \ldots$, its model is of the form

$$D(s) = \prod_{i=1}^{\gamma/2} (s^2 + \omega_i^2).$$

Let ρ be the differential operator defined as $\rho f(t) = \frac{\mathrm{d}f(t)}{\mathrm{d}t}$ and $D(\rho)$ be the corresponding polynomial to the denominator of the disturbance model in ρ, where $\rho^k f(t) = f^{(k)}(t)$ (the k-th derivative of $f(t)$). Then, in the time domain, the input disturbance $\mu(t)$ is described by the following differential equation with $D(\rho)$:

$$D(\rho)\mu(t) = (\rho^\gamma + d_1 \rho^{\gamma-1} + d_2 \rho^{\gamma-2} + \cdots + d_\gamma)\mu(t) = 0. \tag{4}$$

From the internal model control principle, it is known that the feedback control system completely compensates the effect of the periodic disturbance if the controller contains the disturbance model $D(s)$ (Francis and Wonham 1976). The question now is how to embed this model in the continuous time predictive control when orthogonal basis functions (Wang 2009) are used to represent the control trajectory.

Define the following auxiliary variables using the disturbance model:

$$\begin{aligned} z(t) &= D(\rho) x_m(t) \\ u_s(t) &= D(\rho) u(t) \end{aligned} \tag{5}$$

i.e. $z(t)$ and $u_s(t)$ are obtained by filtering the state vector $x_m(t)$ and the control signal $u(t)$, respectively, by the denominator of the transfer-function description of the disturbance model. Also applying the differential operator $D(\rho)$ to both sides of the state equation in the system model (1) gives

$$D(\rho)\dot{x}_m(t) = A_m D(\rho) x_m(t) + B_m D(\rho) u(t) + \Omega_m D(\rho)\mu(t)$$

or

$$\dot{z}(t) = A_m z(t) + B_m u_s(t) \tag{6}$$

where the relation $D(\rho)\mu(t) = 0$ has been used. Similarly, application of $D(\rho)$ to both sides of the output equation in (2) gives

$$D(\rho)\, y(t) = C_m z(t)$$

or

$$\begin{aligned} y^{(\gamma)}(t) = &-d_1 y^{(\gamma-1)}(t) - d_2 y^{(\gamma-2)} - \cdots - d_{\gamma-1}\dot{y}(t) \\ &- d_\gamma y(t) + C_m z(t) \end{aligned} \tag{7}$$

where $y^{(n)}$ denotes the n-th derivative of y.

To obtain state-space model that embeds the disturbance model, choose the new state vector as

$$x(t) = \begin{bmatrix} z(t)^T & y^{(\gamma-1)}(t) & y^{(\gamma-2)} & \ldots & \dot{y}(t) & y(t) \end{bmatrix}^T$$

leading to the augmented state-space model

$$\begin{aligned} \dot{x}(t) &= Ax(t) + Bu_s(t) \\ y(t) &= Cx(t) \end{aligned} \tag{8}$$

where

$$A = \begin{bmatrix} A_m & O & O & \ldots & O & O \\ C_m & -d_1 & -d_2 & \ldots & -d_{\gamma-1} & -d_\gamma \\ O^T & 1 & 0 & \ldots & 0 & 0 \\ \ldots & \ddots & & & & \\ O^T & 0 & \ldots & 1 & 0 & 0 \\ O^T & 0 & \ldots & 0 & 1 & 0 \end{bmatrix}, \quad B = \begin{bmatrix} B_m \\ 0 \\ 0 \\ \vdots \\ 0 \\ 0 \end{bmatrix}$$

$$C = \begin{bmatrix} 0 & 0 & 0 & \ldots & 0 & 1 \end{bmatrix}$$

and O denotes the $n_1 \times 1$ zero vector.

The structure of the augmented model remains unchanged when the plant is multi-input and multi-output except that (i) the O vector becomes zero matrix with appropriate dimensions, (ii) the scalar coefficients $-d_1, -d_2, \ldots$ are replaced by $-d_1 I, -d_2 I, \ldots$ matrices with appropriate dimensions and (iii) the number 1 is replaced by the identity matrix with compatible dimensions. The key task in the design of the continuous-time model predictive control is to model the auxiliary control signal $u_s(t)$ using a set of orthogonal basis functions.

2.2 *Predicted response*

Suppose that we have m control signals and, for a given prediction horizon T_p and $0 \le \tau \le T_p$, let the filtered control signal be expressed as

$$u_s(\tau) = [u_s(\tau)^1 \; u_s(\tau)^2 \; \ldots \; u_s(\tau)^m]^T$$

and partition the input matrix in the plant state-space model as

$$B = [B^1 \; B^2 \; \ldots \; B^m]$$

where $u_s(\cdot)^i$ is its filtered control signal and B^i is the i-th column of the B matrix. Consider also a stable control system with periodic exogenous signals where the control signal $u(\cdot)$ has periodic components. Then the filtered control $u_s(\cdot)$ only has exponentially decaying modes and the key task in the design of the continuous-time predictive control is to ensure stability within one optimisation window of duration T_p where the filtered control signal $u_s(\tau)$ also has only exponentially decaying modes. When this is achieved, the i-th control signal $u_s(\tau)^i$ $(i = 1, 2, \ldots, m)$ can be described using a set of Laguerre functions as

$$u_s^i(\tau) = L(\tau)^T \eta_i$$

where $L(\tau)^T = [l_1(\tau)\, l_2(\tau) \ldots l_N(\tau)]$ and $\eta_i = \left[\xi_1^i \; \xi_2^i \; \ldots \; \xi_N^i\right]^T$. More specifically, the set of Laguerre functions are defined explicitly by the following differential equation with initial condition $L(0) = \sqrt{2p}\underbrace{[1\,1\,\ldots\,1]^T}_{N}$

$$\dot{L}(\tau) = A_p L(\tau) \tag{9}$$

where

$$A_p = \begin{bmatrix} -p & 0 & \ldots & 0 \\ -2p & -p & \ldots & 0 \\ \vdots & \vdots & \ddots & 0 \\ -2p & \ldots & -2p & -p \end{bmatrix}.$$

Here the parameter p is a scaling factor and N denotes the number of terms used in the orthogonal expansion. The set of Laguerre functions will have a different response time if the scaling factor p is varied but p and N can be selected for each individual input signal in the design.

With this formulation, we compute the prediction of state variables. The model used in the prediction is based on (8) and the input signal is the filtered control. We assume that at the current time, t_i, the state variable vector $x(t_i)$ is available, but if not then an observer is needed to access the state information through the measurement of input and output signals, which will be discussed later. With this setup at the future time $\tau, \tau > 0$, the predicted state variable $x(t_i + \tau \mid t_i)$ is described by the following equation:

$$x(t_i + \tau | t_i) = e^{A\tau} x(t_i) + \int_0^\tau e^{A(\tau-\gamma)} B u_s(\gamma) \mathrm{d}\gamma. \tag{10}$$

Describing the control $u_s(\gamma)$ using the Laguerre functions enables the predicted future state at time τ parameterised by η to be written as

$$\begin{aligned} x(t_i + \tau | t_i) &= e^{A\tau} x(t_i) + \int_0^\tau e^{A(\tau-\gamma)} \\ &\quad \times \left[B^1 L(\gamma)^T B^2 L(\gamma)^T \ldots B^m L(\gamma)^T \right] \mathrm{d}\gamma \eta \\ &= e^{A\tau} x(t_i) + \left[I_{int}(\tau)^1 \, I_{int}(\tau)^2 \ldots I_{int}(\tau)^m \right] \\ &\quad \times \begin{bmatrix} \eta_1 \\ \eta_2 \\ \vdots \\ \eta_m \end{bmatrix} \end{aligned} \tag{11}$$

where $I_{int}(\tau)^i$ is the analytical solution of the i-th integral equation given by the algebraic equation

$$A I_{int}(\tau)^i - I_{int}(\tau)^i A_p^T = -B_i L(\tau)^T + e^{A\tau} B_i L(0)^T. \tag{12}$$

Moreover, the state matrix for the Laguerre functions A_p is a lower triangular matrix and hence (12) has a closed-form solution in the form of a set of linear equations (Wang 2001, 2009).

2.3 *Set-point following of periodic signals*

In the formulation of the augmented model so far in this article, the derivatives of the output have been used in the augmented state variable $x(t)$ (see (8)). If the number of periodic modes is $\gamma/2$, then the output derivatives that will be predicted are $y^{(\gamma-1)}(t)$, $y^{(\gamma-2)}(t), \ldots, \dot{y}(t)$. The predicted output derivatives can be represented using a matrix formulation as below (where we assume a single output for notational simplicity).

Let C_2 be the $\gamma \times (n_1 + \gamma)$ matrix defined by

$$C_2 = \left[o_{n1} \quad I_\gamma \right]$$

where o_{n1} is a zero matrix with the dimension $\gamma \times n_1$ and I_γ is the identity matrix with dimension $\gamma \times \gamma$. Hence the prediction of plant output and its derivatives can be written as

$$\begin{bmatrix} y^{(\gamma-1)}(t_i+\tau|t_i) \\ \vdots \\ \dot{y}(t_i+\tau|t_i) \\ y(t_i+\tau|t_i) \end{bmatrix} = C_2 x(t_i+\tau|t_i) = C_2 e^{A\tau} x(t_i) + \phi(\tau)^T \eta$$

$$\phi(\tau) = C_2 I_{int}(\tau) \tag{13}$$

where $I_{int}(\tau) = [\ I_{int}(\tau)^1\ I_{int}(\tau)^2 \ldots I_{int}(\tau)^m\ ]$. Note that the predicted plant output and its derivative are expressed in terms of the coefficient vector η.

Suppose that at time t_i, the set-point signal $r(t)$ is differentiable up to order $\gamma-1$, and that these variables remain constant within one optimisation window. Then in order to achieve perfect set-point following of the periodic signals, the design objective is to find the control law that will drive the predicted plant output $y(t_i+\tau\,|\,t_i)$ and the predicted derivatives of the plant output as close as possible, in a least squares sense, to the future set-point $r(t_i)$ and the corresponding derivatives.

To proceed with the design, define the error signal vector as

$$e(t_i+\tau|t_i) = \begin{bmatrix} r^{(\gamma-1)}(t_i) - y^{(\gamma-1)}(t_i+\tau|t_i) \\ \vdots \\ \dot{r}(t_i) - \dot{y}(t_i+\tau|t_i) \\ r(t_i) - y(t_i+\tau|t_i) \end{bmatrix}$$

and associated cost function

$$J = \int_0^{T_p} e(t_i+\tau|t_i)^T Q_e e(t_i+\tau|t_i)\,\mathrm{d}\tau + \int_0^{T_p} u_s(\tau)^T R u_s(\tau)\mathrm{d}\tau \tag{14}$$

where Q_e and R are symmetric positive definite and positive semi-definite matrices, respectively (written as $Q>0$ and $R\geq 0$). Also the orthogonal property of the Laguerre functions enables J to be written in the equivalent form

$$J = \int_0^{T_p} e(t_i+\tau|t_i)^T Q_e e(t_i+\tau|t_i)\,\mathrm{d}\tau + \eta^T R_L \eta \tag{15}$$

where $R_L = \mathrm{diag}\{R^i\}$ and $R^i = \lambda_i I_{N_i \times Ni}$ (the $N_i \times N_i$ identity matrix). Note also that

$$e(t_i+\tau|t_i) = \begin{bmatrix} r^{(\gamma-1)}(t_i) \\ \vdots \\ r(t_i) \end{bmatrix} - C_2 e^{A\tau} x(t_i) - \phi(\tau)^T \eta$$

and on defining

$$w(\tau|t_i) = \begin{bmatrix} r^{(\gamma-1)}(t_i) \\ \vdots \\ r(t_i) \end{bmatrix} - C_2 e^{A\tau} x(t_i) \tag{16}$$

the quadratic cost function (15) can be written in the following standard form:

$$J = \eta^T \left\{ \int_0^{T_p} \phi(\tau) Q_e \phi(\tau)^T \mathrm{d}\tau + R_L \right\} \eta - 2\eta^T \int_0^{T_p} \phi(\tau) Q_e w(\tau|t_i) \mathrm{d}\tau + \int_0^{T_p} w(\tau|t_i)^T Q_e w(\tau|t_i) \mathrm{d}\tau \tag{17}$$

which can be written explicitly in terms of set-point signal $r(t_i)$, its derivatives $r^{(\gamma-1)}(t_i), \ldots, \dot{r}(t_i)$ and the state vector $x(t_i)$ as

$$J = \eta^T \Omega \eta - 2\eta^T \left\{ \Psi_1 \begin{bmatrix} r^{(\gamma-1)}(t_i) \\ \vdots \\ r(t_i) \end{bmatrix} - \Psi_2 x(t_i) \right\} + \int_0^{T_p} w(\tau|t_i)^T Q_e w(\tau|t_i)\,\mathrm{d}\tau \tag{18}$$

where

$$\Omega = \int_0^{T_p} \phi(\tau) Q_e \phi(\tau)^T\,\mathrm{d}\tau + R_L$$

$$\Psi_1 = \int_0^{T_p} \phi(\tau) Q_e\,\mathrm{d}\tau; \quad \Psi_2 = \int_0^{T_p} \phi(\tau) Q_e C_2 e^{A\tau}\,\mathrm{d}\tau.$$

Minimisation of (18) without hard constraints on the variables is given by the simple least squares solution:

$$\eta = \Omega^{-1} \left\{ \Psi_1 \begin{bmatrix} r^{(\gamma-1)}(t_i) \\ \vdots \\ r(t_i) \end{bmatrix} - \Psi_2 x(t_i) \right\} \tag{19}$$

and the optimal parameter vector, η, and the optimal control $u_s(\tau)$, $0 \leq \tau \leq T_p$, can be reconstructed using the Laguerre functions as

$$u_s(\tau) = \left[u_s^1(\tau)\, u_s^2(\tau)\ \ldots\ u_s^m(\tau) \right]^T = \begin{bmatrix} L(\tau)^T & o_L & \ldots & o_L \\ o_L & L(\tau)^T & \ldots & o_L \\ \vdots & & & \\ o_L & o_L & \ldots & L(\tau)^T \end{bmatrix} \begin{bmatrix} \eta_1 \\ \eta_2 \\ \vdots \\ \eta_m \end{bmatrix} \tag{20}$$

where o_L is a zero vector of dimension $1 \times N$.

By applying the principle of receding horizon control (i.e. the control action will use only the

information $u_s(\tau)$ at $\tau=0$), the optimal control $u_s(t)$ for the unconstrained problem at time t_i is

$$u_s(t_i)=\begin{bmatrix} L(0)^T & o_L & \dots & o_L \\ o_L & L(0)^T & \dots & o_L \\ \vdots & & & \\ o_L & o_L & \dots & L(0)^T \end{bmatrix}\Omega^{-1} \times\left\{\Psi_1\begin{bmatrix} r^{(\gamma-1)}(t_i) \\ \dots \\ r(t_i)\end{bmatrix}-\Psi_2 x(t_i)\right\}. \quad (21)$$

Also define K from (21) as

$$K=\begin{bmatrix} L(0)^T & o_L & \dots & o_L \\ o_L & L(0)^T & \dots & o_L \\ \vdots & & & \\ o_L & o_L & \dots & L(0)^T \end{bmatrix}\Omega^{-1}\Psi_2. \quad (22)$$

Then the closed-loop state matrix is

$$A_{cl}=A-BK \quad (23)$$

from which we can assess the closed-loop performance of the predictive control system when constraints are not imposed.

In this design, the Laguerre scaling parameter p and the number of terms used, N, are the performance tuning parameters. When N is large, with a long prediction horizon T_p, the filtered control trajectory $u_s(\cdot)$ closely matches the underlying optimal control trajectory defined by the linear quadratic regulator (LQR) (Wang 2009), where equivalently the weighting matrices $Q=C_2^TQ_eC_2$ and R remain unchanged. The small discrepancy here is caused by the fact that the design model A contains sinusoidal modes, leading to numerical errors when computing the matrices Ω, Ψ_1 and Ψ_2 using a long prediction horizon. These numerical errors can be removed if modified matrices A_α and Q_α are used in the computation, where A_α and Q_α are given by

$$A_\alpha=A-\alpha I;\quad Q_\alpha=Q+2\alpha P \quad (24)$$

where $\alpha>0$ is selected such that all eigenvalues of A_α lie in the open left-half of the complex plane, and $P>0$ is the solution of the Riccati equation

$$PA+A^TP-PBR^{-1}B^TP+Q=0. \quad (25)$$

2.4 *Control implementation*

The information about the optimal $u_s(t)$ at time t_i needs to be converted to the actual control signal $u(t)$ at t_i for control implementation. In order to achieve this conversion, we use the relationship between the two signals, which is $u_s(t)=D(\rho)u(t)$. Also defining

$$U(t)=\begin{bmatrix} u^{(\gamma-1)}(t) & u^{(\gamma-2)}(t) & \dots & \dot{u}(t) & u(t)\end{bmatrix}$$

and using a controller canonical form realisation gives

$$\dot{U}(t)=A_uU(t)+B_uu_s(t) \quad (26)$$

where

$$A_u=\begin{bmatrix} -d_1 & -d_2 & \dots & -d_{\gamma-1} & -d_\gamma \\ 0 & 1 & \dots & 0 & 0 \\ \dots & \ddots & & & \\ 0 & \dots & 1 & 0 & 0 \\ 0 & 0 & \dots & 1 & 0 \end{bmatrix},\quad B_u=\begin{bmatrix} 1 \\ 0 \\ \vdots \\ 0 \\ 0\end{bmatrix}$$

Moreover, approximating the differential equation (26) with sampling interval Δt gives the optimal control at t_i as

$$U(t_i)=(I-A_u\Delta t)^{-1}U(t_{i-1})+(I-A_u\Delta t)^{-1}B_uu_s(t_i)\Delta t \quad (27)$$

where the backward difference approximation, $\frac{df(t)}{dt}|_{t=t_i}\approx\frac{f(t_i)-f(t_{i-1})}{\Delta t}$, is used. The actual control $u(t_i)$ is computed using the optimal signal $u_s(t_i)$ and the previous states of the control derivatives and the control itself.

Note that in this formulation the computation of the actual control vector is iterative. At the instant when the control system is switched on, the initial conditions of the control vector are specified, i.e. $U(t_0)$. These can be chosen to correspond to the actual plant control states. For instance, the control signal $u(t_0)$ is chosen to be equal to the actual input to the plant and the derivatives of $u(t)$ equal to zero. With this selection, the recursive computation will automatically update the actual control signal to the plant, and the implementation of the control system is performed without additional information, such as plant steady-state value.

The resulting state-space model here contains the auxiliary state variable vector $z(t), y(t)^{(\gamma-1)},\dots,\dot{y}(t)$ and $y(t)$ which involves the derivatives of the original state variable vector $x_m(t)$ and output $y(t)$, and it is not desirable to implement the continuous-time predictive controller using $z(t)$ even if $x_m(t)$ is available. This is because differentiation of a signal will amplify existing measurement noise in the system. Instead, an observer is proposed to estimate the augmented state vector $x(t)$, regardless of whether or not the original state vector $x_m(t)$ is available or not. The observer will have a structure that matches the augmented model in

the form:

$$\frac{\mathrm{d}\hat{x}(t)}{\mathrm{d}t} = A\hat{x}(t) + Bu_s(t) + K_{ob}(y(t) - \hat{y}(t)) \tag{28}$$

where $\hat{x}(t)$ and $\hat{y}(t)$ are the estimated state variable and output, respectively, and K_{ob} is the observer gain matrix.

2.5 *Constrained control*

The main strength of model predictive control lies in its ability to incorporate hard constraints in the design with on-line optimisation. The hard constraints on the derivatives of the control and the control itself are frequently encountered and formulated as follows, where for notational simplicity we assume a single input signal $u(t)$ and consider putting constraints on the first sample of the optimal signals (i.e. $\tau = 0$).

From (27), we can express $\dot{u}(t_i)$ and $u(t_i)$ as functions of the parameter vector η ($u_s(t_i) = L(0)^T\ \eta$). In particular, defining the matrix C_s as

$$C_s = \begin{bmatrix} 0 & \dots & 0 & 1 & 0 \\ 0 & \dots & 0 & 0 & 1 \end{bmatrix}$$

the vector $[\dot{u}(t_i)\, u(t_i)]^T$ has the following relationship with the Laguerre parameter vector η

$$\begin{bmatrix} \dot{u}(t_i) \\ u(t_i) \end{bmatrix} = C_s(I - A_u\Delta t)^{-1}U(t_{i-1}) + C_s(I - A_u\Delta t)^{-1}B_u\Delta t L(0)^T\eta. \tag{29}$$

Assume that the hard constraints on $\dot{u}(t)$ and $u(t)$ are $\dot{u}^{\min} \le \dot{u}(t) \le \dot{u}^{\max}$ and $u^{\min} \le u(t) \le u^{\max}$, respectively, or

$$\begin{bmatrix} \dot{u}^{\min} \\ u^{\min} \end{bmatrix} \le \begin{bmatrix} \dot{u}(t_i) \\ u(t_i) \end{bmatrix} \le \begin{bmatrix} \dot{u}^{\max} \\ u^{\max} \end{bmatrix}. \tag{30}$$

In terms of the Laguerre parameter vector η, the set of linear inequality constraints that will be used in the optimisation problem are

$$-C_s(I - A_u\Delta t)^{-1}B_u\Delta t L(0)^T\eta \le C_s(I - A_u\Delta t)^{-1}U(t_{i-1}) - \begin{bmatrix} \dot{u}^{\min} \\ u^{\min} \end{bmatrix} \tag{31}$$

$$C_s(I - A_u\Delta t)^{-1}B_u\Delta t L(0)^T\eta \le -C_s(I - A_u\Delta t)^{-1}U(t_{i-1}) + \begin{bmatrix} \dot{u}^{\max} \\ u^{\max} \end{bmatrix} \tag{32}$$

and the predictive control problem with hard constraints imposed on the design becomes that of finding the optimal solution of the quadratic cost function

$$J = \eta^T\Omega\eta - 2\eta^T\left\{\Psi_1\begin{bmatrix} \dot{r}(t_i) \\ r(t_i) \end{bmatrix} - \Psi_2 x(t_i)\right\} + \int_0^{T_p} w(\tau|t_i)^T Q_e w(\tau|t_i)\,\mathrm{d}\tau \tag{33}$$

subject to the linear inequality constraints (31) and (32). This is a standard constrained quadratic minimisation problem, and the optimal solution can be found using a quadratic programming algorithm, such as that in Wang (2009).

2.6 *Switched linear controllers*

In the approach to the design of the model predictive control for the periodic signals developed above, the frequencies of either the reference or disturbance signal are embedded in the design. In addition, the derivatives of the reference signal up to the order of $\gamma - 1$ are needed. There are some applications where the reference signals are only piece-wise differentiable. In such cases, the reference trajectory can be divided into several pieces with each being differentiable up to the order of $\gamma - 1$. As the reference trajectory changes, the predictive controller will be effectively switched from one to another. This leads to a switched linear controller implementation.

The receding horizon control principle that has been used in the design gives a natural setting for a switched linear controller. With this framework, there are a set of the cost functions pre-computed using the augmented model structure (8) according to the frequency content of the reference trajectory. Each cost function corresponds to a single piece of the trajectory, within which the reference signal is assumed to be differentiable up to the order of $\gamma - 1$, and the predictive controller in real-time minimises the cost function subject to constraints. When the trajectory changes, the cost function is switched to the form which reflects the appropriate frequency contents contained in the reference. An example is given in the section below to demonstrate this switching controller option.

Since the predictive control law is changed from one to another when the reference trajectory changes, the corresponding signal $u(t)$ could potentially become discontinuous at the point of switching, which should be avoided in practical applications. This is naturally resolved since $u(t)$ is guaranteed to be continuous at the point of switching when the sampling interval $\Delta t \to 0$,

which follows from

$$\lim_{\Delta t\to 0} U(t_i) = \lim_{\Delta t\to 0}(I - A_u\Delta t)^{-1}U(t_{i-1}) + \lim_{\Delta t\to 0}(I - A_u\Delta t)^{-1}B_u u_s(t_i)\Delta t = U(t_{i-1}). \quad (34)$$

3. Examples

This section will demonstrate in simulation performance achievable from the continuous-time predictive control algorithm developed above. We will show the cases of unconstrained control and constrained control, respectively. The system used for these is a power electronic device with state-space model

$$\dot{x}_m(t) = A_m x_m(t) + B_m u(t), \quad y(t) = C_m x_m(t) \quad (35)$$

where

$$A_m = \begin{bmatrix} 0 & -2.6667\times 10^3 \\ 80 & -66.6667 \end{bmatrix}, \quad B_m = \begin{bmatrix} 2\times 10^5 \\ -25 \end{bmatrix}$$
$$C_m = \begin{bmatrix} 0 & 1 \end{bmatrix}.$$

This system is severely under-damped, which has a pair of complex modes $\lambda_1 = -33.3333 + i460.6758$, $\lambda_2 = -33.3333 - i460.6758$.

3.1 *Set-point following with constraints*

Assume that the set-point signal is a ramp $\omega_0 = 0$ followed by a sinusoidal input signal with frequency $\omega_0 = 2.8$, and we also assume that these signals have a smooth transition from one to the other. The design objective is that the output follows the reference signal as close as possible subject to the following constraints on the amplitude of the control signal:

$$-0.015 \le u(t) \le 0.015.$$

For a comparison, we simulate three cases: without constraints, predictive control with embedded constraints and state feedback control with saturation, respectively.

We include these two frequencies ($\omega_0 = 0$ and $\omega_0 = 2.8$ rad/s in the design of model predictive control to obtain two sets of control parameter matrices for the quadratic cost function (33). The observer is also designed using these two frequencies. The control law automatically switches when the set-point signal changes its frequency.

The parameters for the continuous-time predictive control are chosen as $p = 63$, $N = 3$, $T_p = 0.4762$, $Q_e = C_2^T C_2$ and $R = 0.0001$. Here p is chosen around twice the modulus of the real part of the open-loop poles.

The control law for the ramp signal is determined by minimising the cost function (33). For $\omega_0 = 0$,

$$\Omega = \begin{bmatrix} 5.7985 & -5.1993 & 4.6071 \\ -5.1993 & 4.6799 & -4.1606 \\ 4.6071 & -4.1606 & 3.7155 \end{bmatrix}$$
$$\Psi_1 = \begin{bmatrix} 0.4567 & 1.4159 \\ -0.4089 & -1.2275 \\ 0.3618 & 1.0525 \end{bmatrix}$$
$$\Psi_2 = \begin{bmatrix} 0.0002 & 0.0000 & 0.4567 & 1.4159 \\ -0.0002 & -0.0000 & -0.4089 & -1.2275 \\ 0.0001 & 0.0000 & 0.3618 & 1.0525 \end{bmatrix}$$

For $\omega_0 = 2.8$ rad/s

$$\Omega = \begin{bmatrix} 4.1445 & -3.7968 & 3.4261 \\ -3.7968 & 3.4985 & -3.1728 \\ 3.4261 & -3.1728 & 2.8957 \end{bmatrix}$$
$$\Psi_1 = \begin{bmatrix} 0.3227 & 0.7467 \\ -0.2950 & -0.6362 \\ 0.2655 & 0.5339 \end{bmatrix}$$
$$\Psi_2 = \begin{bmatrix} 0.0001 & 0.0000 & 0.3227 & 0.7467 \\ -0.0001 & -0.0000 & -0.2950 & -0.6362 \\ 0.0001 & 0.0000 & 0.2655 & 0.5339 \end{bmatrix}$$

and these laws are different. The observer for each case has been designed using the pole-placement method, where the desired closed-loop poles are selected as -189.0000, -189.5000, -190.0000, -190.5000, roughly located at $-3\times p$.

The closed-loop system is simulated using a sampling interval of 0.00005 s. Without constraints, the closed-loop output response and the set-point signal are compared in Figure 1(a). It is seen that the output tracks the set-point signal very closely. In fact the absolute maximum tracking error occurred at the transition point between the two set-point signals, and has a value of 0.049.

When the constraints are imposed in the design, the predictive control finds the optimal control signal subject to the constraints (Figure 1(b)). For comparison purposes, we simulated the case when a saturation of the control amplitude is used, instead of using the predictive control scheme. Figure 2 shows the simulation results. It is seen that the tracking performance degrades when the control signal amplitude is constrained at 0.015, and control system is not able to recover after the saturation is introduced.

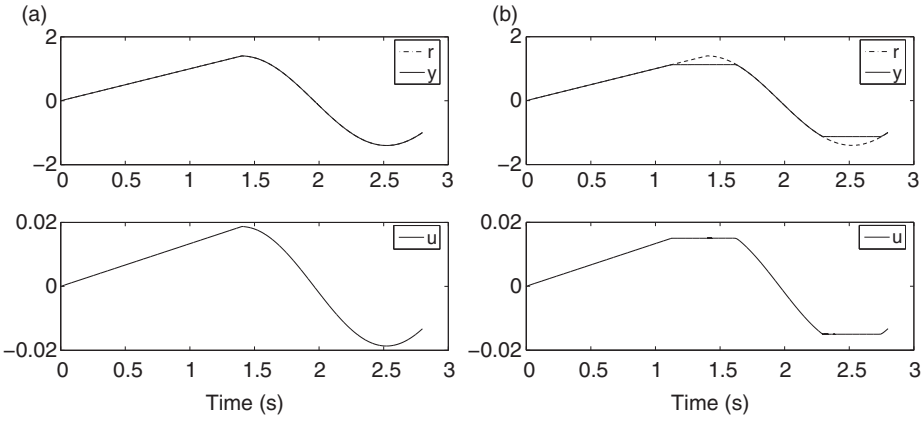

Figure 1. Comparison of predictive control with and without constraints: set-point following case: (a) tracking of the reference and (b) tracking of the reference with constraints.

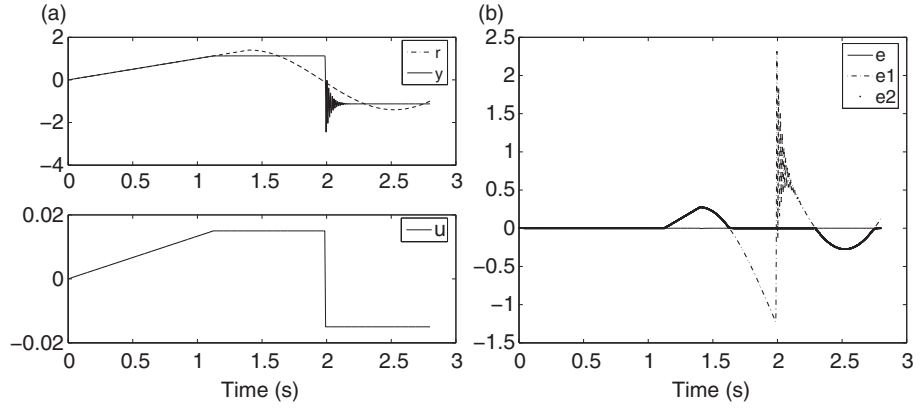

Figure 2. Comparison results: (a) tracking of the reference with saturation and (b) comparison of the tracking errors.

3.2 *Disturbance rejection with constraints*

To illustrate rejection of input disturbance we introduce the signal to be rejected as two sinusoidal signals with $\omega_0 = 60$ and $\omega_0 = 6$ rad/s. The disturbance signal is added to the control signal, and a white noise with 0.1 standard deviation is added to the output to simulate the existing measurement noise. The design parameters for the predictive control system are identical to the ones used in the set-point following case, except that the frequency parameters are different. The constraints on the control amplitude are specified as $-1.1 \leq u(t) \leq 1.1$. Figure 3 shows the simulation results with constraints.

4. Gantry robot example

This section shows the results from a case study where the plant transfer function has been obtained from tests on a gantry robot undertaking pick and place operations. The results presented here are simulated, and experimental implementation is currently under way.

4.1 *Process description*

The gantry robot, shown in Figure 4, is a commercially available system found in a variety of industrial applications whose task is to place a sequence of objects onto a moving conveyor under synchronisation. The sequence of operations is that the robot collects the object from a specified location, moves until it is synchronised (in terms of both position and speed) with the conveyor, places the object on the conveyor, and then returns to the same starting location to collect the next object and so on. This experimental facility has been extensively used in the benchmarking of repetitive and iterative learning control algorithms; see, for example, Ratcliffe (2005), Ratcliffe, Lewin, Rogers, Hatonen, and Owens (2006)

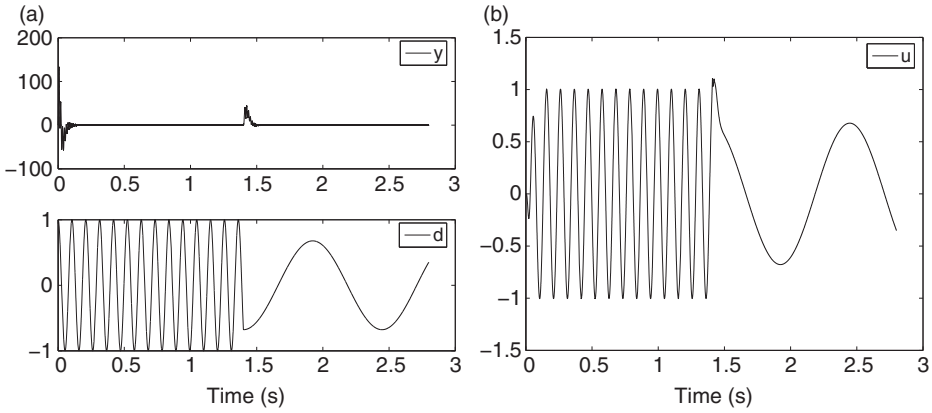

Figure 3. Predictive control with constraints. Input disturbance rejection case in the presence of measurement noise: (a) output and disturbance and (b) control signal.

Figure 4. The gantry robot.

and Ratcliffe, Hatonen, Lewin, Rogers, and Owens (2007, 2008).

The gantry robot can be treated as three SISO systems (one for each axis) which can operate simultaneously to locate the end effector anywhere within a cuboid work envelope. The lowest axis, X, moves in the horizontal plane, parallel to the conveyor beneath. The Y-axis is mounted on the X-axis and moves in the horizontal plane, but perpendicular to the conveyor. The Z-axis is the shorter vertical axis mounted on the Y-axis. The X- and Y-axes consist of linear brushless dc motors, while the Z-axis is a linear ball-screw stage powered by a rotary brushless dc motor. All motors are energised by performance matched dc amplifiers. Axis position is measured by means of linear or rotary optical incremental encoders as appropriate.

To obtain a model for the plant which is to be controlled, each axis of the gantry was modelled independently by means of sinusoidal frequency response tests. From this data it was possible to construct the Bode plots for each axis and hence determine approximate transfer functions. These were then refined, by means of a least mean squares optimisation technique, to minimise the difference between the frequency response of the real plant and that of the model. The resulting X-axis Bode plot comparing the plant and the model is given in Figure 5 (the remaining plots appear in Ratcliffe (2005)). From each Bode plot an approximate transfer function was constructed and from that, a minimal order state-space model. Here we only consider the X-axis where a 7-order transfer function was used in design, where the Laplace transfer function is given as

$$G(s) = \frac{\left\{\begin{array}{l}(s+500.19)(s+4.90\times10^5)\\ \quad\times(s+10.99\pm j169.93)(s+5.29\pm j106.86)\end{array}\right\}}{\left\{\begin{array}{l}s(s+69.74\pm j459.75)(s+10.69\\ \quad\pm j141.62)(s+12.00\pm j79.10)\end{array}\right\}}. \tag{36}$$

4.2 *Determination of the disturbance model*

The reference signal over one period has 200 samples and the X-axis component is shown in Figure 6(a). With the sampling interval of 0.01 s, the period of this signal is $T=2$ (s). From this reference signal, the dominant frequencies contained are determined, leading to the disturbance model $D(s)$ required for the design.

It is a standard fact that a discrete periodic signal $r(k)$ can be uniquely represented by the inverse discrete fourier transform

$$r(k) = \frac{1}{M}\sum_{i=0}^{M-1} R_f(e^{j\frac{2\pi i}{M}})e^{j\frac{2\pi ik}{M}} \tag{37}$$

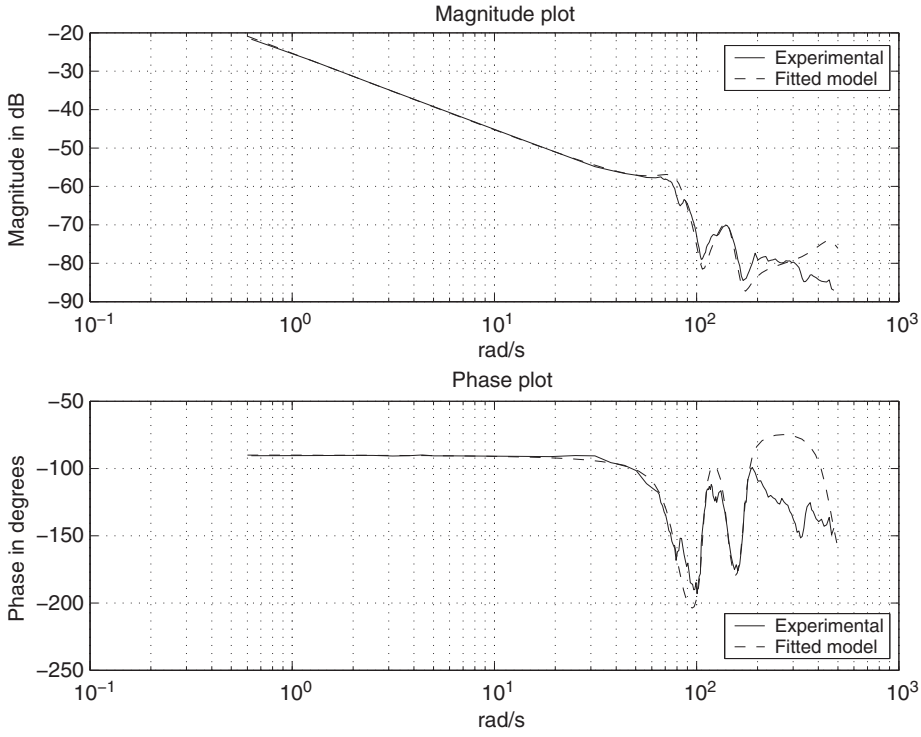

Figure 5. The Bode gain (top) and phase (bottom) plots for the X-axis.

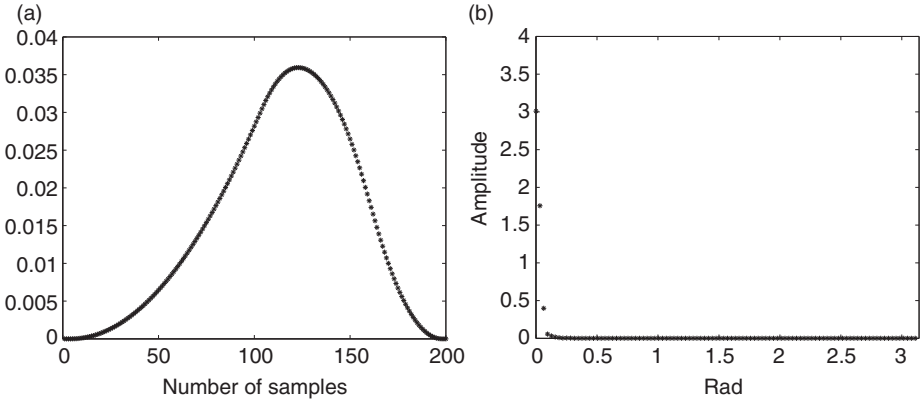

Figure 6. (a) Discrete reference signal and (b) magnitudes of the frequency components.

where M is the number of samples within a period and $R_f(e^{\frac{2\pi i}{M}})$ $(i=0,1,2,\ldots,M-1)$ are the frequency components contained in the periodic signal. For this reference signal, the frequency components $R_f(e^{\frac{2\pi i}{M}})$ where $i=0,1,2,\ldots,M-1$, are obtained via Fourier analysis. The magnitudes of the frequency components are shown in Figure 6(b).

From this last plot we have seen that there are three significant frequencies contained in the signal, at 0, $2\pi/M$ and $4\pi/M$ while the rest of the frequencies are insignificant because of their much smaller magnitudes. Hence the continuous-time frequencies that correspond to the discrete frequencies are $\omega_0=0$, $\omega_1=2\pi/2$ and $\omega_2=4\pi/2$ $(T=M\Delta t)$, respectively. The disturbance model to be embedded in the controller is determined by the three dominant frequencies and is given by

$$D(s)=s(s^2+\pi^2)(s^2+4\pi^2). \tag{38}$$

4.3 *Tuning of the predictive controller*

The performance tuning parameters in this particular case are the weighting matrix Q and the scalar R in the cost function, and the Laguerre parameters p and N. The parameter p has been set at a value close to the

modulus of the real part of the dominant pole and a sufficient large number of N (15) is used so that the predictive control trajectory converges to the trajectory of underlying optimal LQR. However, the augmented model has 12 states and hence is difficult to find the desired performance via the selection of individual elements in Q and the scalar R. (This problem would be compounded for a multi-input multi-output example.)

Suppose the cost function J is selected as

$$J = \int_0^{T_p} (e^{(4)}(t))^2 + (e^{(3)}(t))^2 + (e^{(2)}(t))^2 + (\dot{e}(t))^2 + (e(t))^2 + u_s(t)^T R u_s(t)\,\mathrm{d}t \quad (39)$$

where $e(t) = r(t) - y(t)$ and $e^{(k)}(t)$ denotes the k-th derivative of the error signal. Then in this case Q is a block diagonal matrix, with the first block entry being a 7×7 zero matrix, and the second a 5×5 identity matrix, and $R > 0$. With this selection, the common approach to tuning the closed-loop performance is to select R. After numerous trials, it is found that there are five closed-loop poles, which are difficult to re-assign and form a cluster with a real part around -0.002, despite the selection of R as a very small number ($R = 10^{-5}$), and hence we need to use an advanced tuning method. One such method is given in Wang (2009) for the continuous-time predictive control with a prescribed degree of stability and is now applied to this example.

In this case, the model used in the design has two poles at the origin and two pairs of poles on the imaginary axis and as a result the computation of the predictive controller is ill-conditioned unless exponentially weighted cost is used (Wang 2009). Here we select the weight factor $\alpha = 0.18$ and modify the state matrix of the design model to $A_\alpha = A - \alpha I$, where A is the state matrix from the original augmented model and I is the identity matrix of 12×12. The closed-loop performance is determined by the location of the closed-loop poles where a maximum real part of the closed-loop poles is enforced (i.e. the real parts of the poles are to the left of $-\beta$ where β is a positive scalar). With given Q and R matrices, we solve the following Riccati equation with the parameter β to obtain the matrix P

$$P(A + \beta I) + (A + \beta I)^T P - PBR^{-1}B^T P + Q = 0 \quad (40)$$

and then compute Q_α as

$$Q_\alpha = Q + 2(\alpha + \beta)P.$$

Next, the design procedure of Section 2 is used with Q_α and A_α replacing the Q and A matrices, respectively.

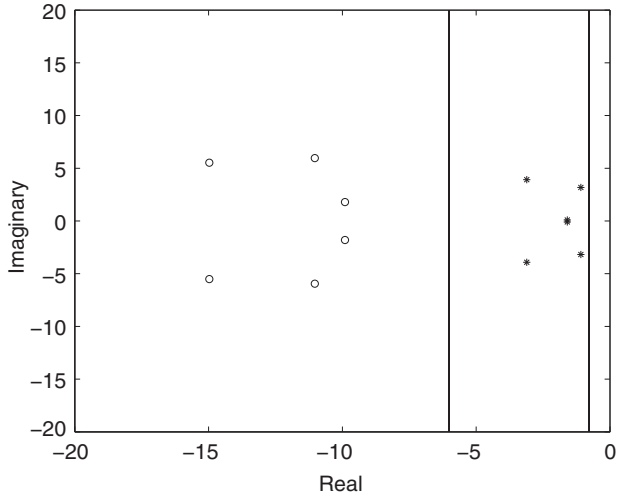

Figure 7. The dominant closed-loop eigenvalues and β line (*, $\beta = 0.8$ and ○, $\beta = 6$).

On completion the predictive control scheme will have a prescribed degree of stability β.

To illustrate the application of this design we consider three cases: $\beta = 0.8$ (Case A); $\beta = 1.8$ (Case B); $\beta = 6$ (Case C). For all the cases, the weight parameter on the control signal $R = 1$. In each case, the closed-loop eigenvalues of the predictive control system are allocated to the left of the line $-\beta$. Figure 7 compares the closed-loop dominant eigenvalues generated from the design with the parameter $\beta = 0.8$ (Case A) and $\beta = 6$ (Case C), respectively. It is seen from this figure that when $\beta = 0.8$, the six closed-loop dominant poles are on the left-hand side of $-\beta = -0.8$ line and when $\beta = 6$, the six closed-loop dominant poles on the left-hand side of $-\beta = -6$ line.

For these designs, the continuous-time closed-loop predictive control system was simulated under fast sampling. Here the sampling rate of $5e^{-5}$ s was used and the original reference trajectory is interpolated with a 8th-order polynomial to achieve such as fast sampling in the simulation. Figure 8 shows both the output of the predictive controller and the position of the robot. Figure 9 compares the tracking errors among the three cases. It is seen that the tracking error converges to zero for all three cases; however, because of the fast dynamic response for Case C, the tracking error is significantly smaller than the other two cases.

5. Conclusions

This article has developed an approach to disturbance rejection and set-point following of the periodic signals in the framework of predictive control with constraints. The predictive control system is designed

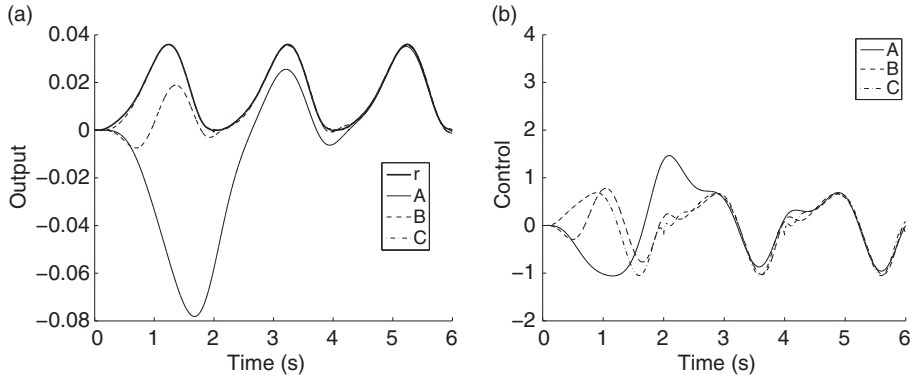

Figure 8. Case A $\beta = 0.8$; case B $\beta = 1.8$; case C $\beta = 6$: (a) tracking of the reference and (b) control signal.

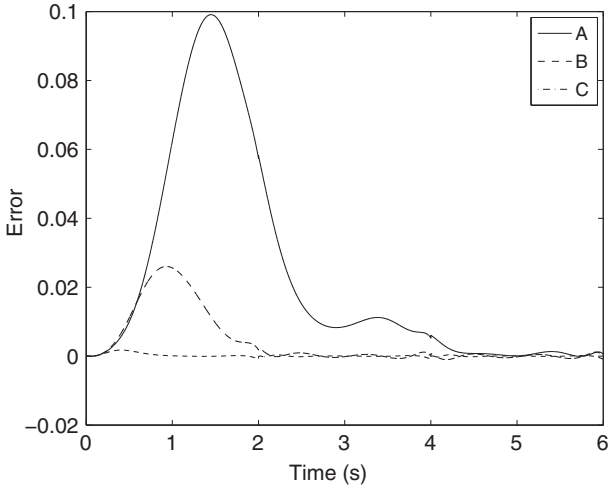

Figure 9. Comparison of tracking errors.

with embedded periodic components in the augmented model where a set of continuous-time Laguerre functions is used to describe the inversely filtered control signal. As a result, the control system tracks (or rejects) sinusoidal signals with zero steady-state errors. The simulation results demonstrate that the predictive control system can produce optimal results with constraints.

Acknowledgements

Peter Gawthrop is a Leverhulme Emeritus Research Fellow and gratefully acknowledges the support of the Leverhulme Trust. The work reported here was accomplished whilst the second author was a Visiting Professor at RMIT University, Melbourne supported by the Australian Advanced Manufacturing Cooperative Research Center (AMCRC). The work reported here is partly supported by the linked EPSRC Grants EP/F068514/1, EP/F069022/1 and EP/F06974X/1 'Intermittent control of man and machine'.

References

Bai, M.R., and Wu, T.Y. (1998), 'Simulation of an Internal Model Based Active Noise Control System for Suppressing Periodic Disturbances', *ASME Journal of Vibration and Acoustics*, 120, 111–116.

Clarke, D.W., Mohtadi, C., and Tuffs, P.S. (1987), 'Generalized Predictive Control: Part 1. The Basic Algorithm: Part 2. Extensions and Interpretations', *Automatica*, 23, 137–160.

Francis, B.A., and Wonham, W.M. (1976), 'The Internal Model Principle of Control Theory', *Automatica*, 12, 457–465.

Garnier, H., and Wang, L. (eds.) (2008), *Continuous-time Model Identification from Sampled Data*, Berlin: Springer Verlag.

Gawthrop, P.J., and Ronco, E. (2002), 'Predictive Pole-placement Control with Linear Models', *Automatica*, 38, 421–432.

Gawthrop, P.J., and Wang, L. (2006), 'Intermittent Predictive Control of an Inverted Pendulum', *Control Engineering Practice*, 14, 1347–1356.

Gawthrop, P.J., and Wang, L. (2009), 'Event-driven Intermittent Control', *International Journal of Control*, 82, 1138–1147.

Hara, S., Yamamoto, Y., Omata, T., and Nakano, M. (1988), 'Repetitive Control System: A New Type Servo System for Periodic Exogenous Signals', *IEEE Transactions on Automatic Control*, 33, 659–668.

Hu, J., and Tomizuka, M. (1993), 'A New Plug-in Adaptive Controller for Rejection of Periodic Disturbances', *Journal of Dynamic Systems, Measurement, and Control*, 115, 543–546.

Li, C., Dongchun, Z., and Xianyi, Z. (2004), 'A Survey of Repetitive Control', in *Proceedings of the 2004 IEEE/RSJ International Conference on Intelligent Robots and Systems, 2004, (IROS 2004)*, Vol 2. pp. 1160–1166.

Maciejowski, J.M. (2002), *Predictive Control with Constraints*, Harlow, UK: Pearson Education Limited.

Manayathara, T.J., Tsao, T.C., Bentsman, J., and Ross, D. (1996), 'Rejection of Unknown Peridoic Load Disturbances in Continuous Steel Casting Process using Learning Repetitive Control Approach', *IEEE Transactions on Control Systems Technology*, 4, 259–265.

Nestorovic-Trajkov, T., Koppe, H., and Gabbert, U. (2005), 'Active Vibration Control using Optimal LQ Tracking System with Additional Dynamics', *International Journal of Control*, 78, 1182–1197.

Owens, D.H., Li, L.M., and Banks, S.P. (2004), 'Multi-periodic Repetitive Control System: A Lyapunov Stability Analysis for Mimo Systems', *International Journal of Control*, 77, 504–515.

Ratcliffe, J.D. (2005), 'Iterative Learning Control Implemented on a Multi-axis System', Ph.D. thesis, University of Southampton.

Ratcliffe, J.D., Hatonen, J.J., Lewin, P.L., Rogers, E., and Owens, D.H. (2007), 'Repetitive Control of Synchronized Operations for Process Applications', *International Journal of Adaptive Control and Signal Processing*, 21, 300–325.

Ratcliffe, J.D., Hatonen, J.J., Lewin, P.L., Rogers, E., and Owens, D.H. (2008), 'Norm-optimal Iterative Learning Control Applied to a Gantry Robots for Automation Applications', *International Journal of Robust and Nonlinear Control*, 18, 1089–1113.

Ratcliffe, J.D., Lewin, P.L., Rogers, E., Hatonen, J.J., and Owens, D.H. (2006), 'Norm-optimal Iterative Learning Control Applied to a Gantry Robots for Automation Applications', *IEEE Transactions on Robotics*, 22, 103–107.

Rawlings, J.B. (2000), 'Tutorial Overview of Model Predictive Control', *IEEE Control Systems Magazine*, 20, 38–52.

Sbarbaro, D., Tomizuka, M., and Leon de la Barra, B. (2009), 'Repetitive Control System under Actuator Saturation and Windup Prevention', *Journal of Dynamic Systems, Measurement and Control*, 131, 044505.

Tomizuka, M., Chew, K.-K., and Yang, W.-C. (1990), 'Disturbance Rejection through an External Model', *Journal of Dynamic Systems, Measurement and Control*, 112, 559–564.

Wang, L. (2001), 'Continuous Time Model Predictive Control using Orthonormal Functions', *International Journal of Control*, 74, 1588–1600.

Wang, L. (2009), *Model Predictive Control System Design and Implementation using MATLAB*, Berlin: Springer-Verlag.